Chalmers Publication Library

Preliminary Investigations of Three-Dimensional Microwave Tomography using Different Data Sets

(article starts on next page)

Preliminary Investigations of Three-Dimensional Microwave Tomography Using Different Data Sets

Hoi-Shun Lui, Andreas Fhager, Mikael Persson
Department of Signals and Systems
Chalmers University of Technology,
Gothenburg, Sweden
antony.lui@chalmers.se

Abstract—**Owing to the extensive amount of computing resources required for solving the non-linear microwave inverse scattering problems, previous numerical studies have mainly been focus on two-dimensional inverse scattering problemw. In three-dimensional cases, the vectorial nature of electromagnetic waves has to be properly handled. In this paper, preliminary investigations of using vertical and horizontal components of the scattered near-field are considered. The forward data is first evaluated quantitatively and image reconstruction using the two different sets of data from the same scattering problem is performed.**

Keywords- microwave breast imaging, inverse scattering, microwave tomography, transient electromagnetic field, ultra wideband imaging

I. INTRODUCTION

Detection and imaging of tumor inside breast using microwave technologies have been of significant interest in the last two decades. Compared to X-ray mammography which is currently used routinely in hospital for breast cancer screening, microwave radiation is non-ionizing which is less harmful to the subject. Under microwave illumination, the dielectric contrast between healthy glandular tissue and malignant tumor is higher as compared to using X-ray [1]. With these motivations in mind, many research groups all over the world have been working on the problem.

In general, there are two ways to approach this problem, namely the radar-based approach [1] and the tomography approach [2]-[3]. The radar-based approach aims to identify the presence and location of the strong scatterer due to the huge contrast between the tumor and the glandular tissue. This involves focusing reflections from the breast volume, which is a coherent-sum process adapted from synthetic aperture radar (SAR) [1]. On the other hand, the tomography approach aims to reproduce the dielectric profiles of the entire breast volume. This involves solving the inverse scattering problem. Due to the huge contrast between the tumor and the glandular tissue, the inverse problem becomes non-linear. Techniques such as filtered back projection developed for X-ray computed tomography cannot be used. For microwave tomography, the problem has to be solved in an iterative manner. A cost function is first defined based on the differences between the measured scattered field of the actual breast volume and the simulated breast volume in the computational domain. In the

computational domain, the breast volume is discretized into a large number of cells (hundreds to thousands) with unknown dielectric profiles (relative permittivity and conductivity). We aim to solve the unknowns in an iterative manner by minimizing the cost function [2]-[3].

Apparently, microwave tomography approach for breast cancer detection is computational extensive that requires many computer memory and long computation time. As a result, early studies have mainly been focus on two dimensional problems, i.e. reconstruction of a slice of the breast volume [2]-[3]. With the rapid development of computer technology and computational electromagnetics, this allows us to work on three-dimensional microwave tomography problems. However, this is not a trivial step to move from two dimensional to three dimensional. First, scattering from the breast volume is a three dimensional problem. The breast volume can be treated as a polarization transformer that depolarizes the incoming electromagnetic wave from one polarization state to another. This concerns issues of (i) how we should illuminate the breast volume and (ii) how we should measure the scattered field. To probe further, this corresponds to what field components to measure (polarization in far field) and thus the choice of antenna elements. Furthermore, the position of the antenna location is another question that we have to answer.

In this paper, preliminary investigations of three-dimensional microwave tomography using different data sets are considered. The breast volume is surrounded by cross-dipole antenna arrays such that both vertical and horizontal field components can be measured. In the forward problem, the vertical and horizontal components of the scattered electric field will be evaluated by comparing between breast volumes with different tumor sizes.

II. MICROWAVE TOMOGRAPHY

The microwave tomography algorithm as described in [2]-[3] will be used in this work. The breast volume is surrounded by a number of antenna elements. Given the time domain scattering data from the actual breast volume of interest, $E_{m,n}^{measured}(t)$, and the simulated scattering electric field, $E_{m,n}^{simulated}(t, \varepsilon_r(i,j,k), \sigma(i,j,k))$, a cost function is defined as

$$F\left(\varepsilon_r(i,j,k),\sigma(i,j,k)\right) = \int_0^T \sum_{m=1}^M \sum_{n=1}^N \left(\left|E_{m,n}^{measured}(t)\right.\right.$$

$$\left.\left. - E_{m,n}^{simulated}\left(t.\varepsilon_r(i,j,k),\sigma(i,j,k)\right)\right|^2\right)dt . \quad (1)$$

Here, $\varepsilon_r(i,j,k)$ are $\sigma(i,j,k)$ the dielectric properties of the assumed breast volume in the simulation environment using Finite Difference Time Domain (FDTD) and (i,j,k) is the index of the Yee cell in the FDTD simulation. M and N are the number of transmitting and receiving antennas respectively and the small letters m and n label the antenna elements. The cost function (1) is minimized using a gradient-based optimization algorithm.
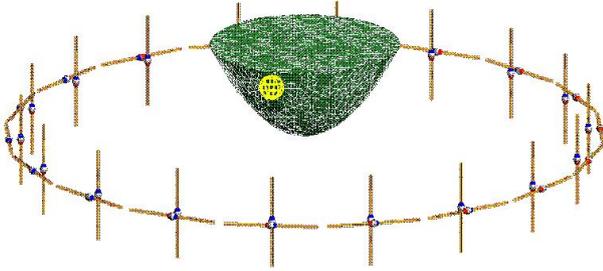
Figure 1. The simulation setup in FEKO environment. The simple breast volume is modelled using a hemisphere (in green) and a tumor is modelled using a small sphere inside the breast (in yellow). The breast volume is surrounded by a circular array of cross dipole antennas.

In previous studies, the reconstruction is performed in two-dimension and only the parallel polarized field is considered. As a proof-of-concept, the scattering problem and the image reconstruction is performed in two-dimension. In the full three-dimensional case, the breast volume acts as a polarization transformer and de-polarizes the incoming field into both horizontal and vertical components even though the incident field is only horizontal or vertical polarized. The vectorial nature of electromagnetic field has to be taken into account when considering the entire inverse scattering problem [4]. In the radar imaging, polarization information has been extensively exploited [5]. Instead of polarization, in the near-field region, we looked into the different field components as a basis for image reconstruction.

III. COMPARISONS OF FORWARD SCATTERING DATA

Before moving into the actual image reconstruction, another question that we need to ask is how well the forward data we can obtain with different field components. In particular, the main objective is to detect malignant tumor inside the breast volume and we need to ensure that the tumor is well illuminated. In view of this, vertical and horizontal field components of the forward scattering problems of the breast volumes with (i) no tumor and (ii) different sizes of tumors are compared quantitatively. This will first give us some ideas about how we should effectively illuminate the breast volume. At the same time, chances for the two different inverse

problems (breast volume with and without tumors) heading to the same solution could potentially be minimized [6]-[7]. In previous work, we have studied the ultra wideband (UWB) scattering of different breast volumes with different tumor sizes and dielectric profiles under plane wave illumination with different polarization basis.
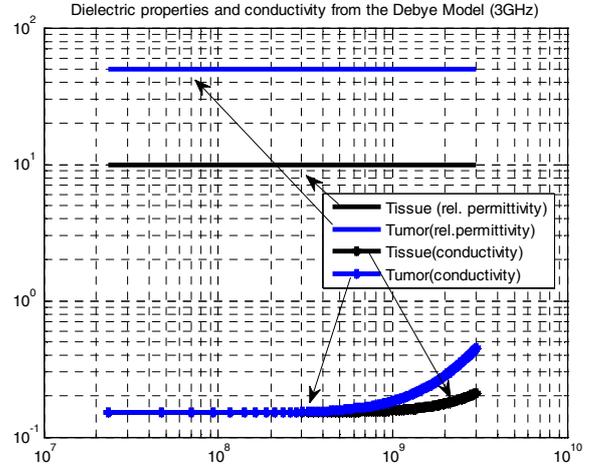
Figure 2. Dielectric Profiles of the breast volume with healthy tissue and tumor using the Debye model [9].
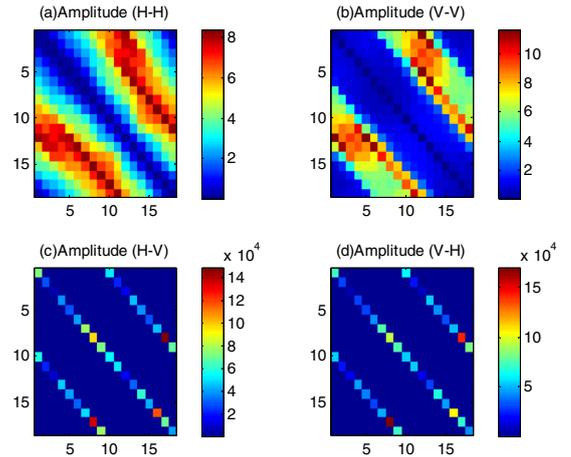
Figure 3. $MD_{A,B,amplitudes}$ values for the case of the 10mm tumor for A and B ranges from 1 to 18, with 1 corresponds to the position of $\varphi = 0°$. (a) to (d) shows the results with different transmitting and receiving antenna pairs that are oriented in (a)Horizontal_Horizontal, (b) Vertical_Vertical, (c) Horizontal_Vertical and (d) Vertical_Horizontal manners.

Instead of exciting the breast volumes under plane wave illumination in [6]-[7], the breast volume is now surrounded by a circular array with cross dipole antennas. Only one antenna is radiating and the scattered field from the breast volume is measured by all the antennas. The electromagnetic problem is solved using commercial hybrid finite element and moment method solver FEKO [8] from 23MHz to 3GHz with 128 samples in frequency domain. The setup in FEKO environment is shown in Fig. 1. The radius of the circular array is 12cm.

Each antenna element is terminated with a 50 ohm load. In total, there are 36 antennas surrounding the breast volume, half of them are oriented vertically and the other half oriented horizontally. The antennas are evenly distributed among the entire circle (i.e. 20° separation). The breast volume is modeled as a hemisphere with a radius of 4cm and the tumor is centered at the position of (r=24.5mm, $\theta = 54.7°$, $\varphi = 45°$). The dielectric properties of the breast volume and the tumor are given by the widely-used Debye model in [9] and the corresponding dielectric profiles are shown in Figure. 2.

In total, there are 36 antenna elements, resulted in 1296 combinations and each of them has 128 frequency samples, which is not easy to analyze individually. In view of this, we need to introduce some parameters to get an overview of the results. As mentioned before, the objective of this work is to quantify the differences of the measured voltages at the antenna terminals (i.e. measurable scattered field components) between breast volumes with and without tumors. Here, we take the case without the tumor as a reference and we compare it for the cases with a tumor with (i) 5mm and (ii) 10mm radius. To quantify the amplitude response, the relative difference and the mean difference between antenna elements A and B are given by $MD_{A,B,amp}$

$$S_{A,B,diff,amplitude}(f) = \frac{\left\| S_{A,B,ref}(f) \right| - \left| S_{A,B,tumor}(f) \right\|}{\left| S_{A,B,ref}(f) \right|} \times 100\% , \quad (2)$$

$$MD_{A,B,amplitude} = \frac{\left[\sum_{f=\Delta f}^{N\Delta f} S_{AB,diff,amplitude}(f) \right]}{N}, \quad (3)$$

where $\left| S_{A,B,ref}(f) \right|$ and $\left| S_{A,B,tumor}(f) \right|$ are the S-parameters of antenna elements A and B for the cases (i) without and (ii) with tumor respectively. The phase information between the two cases are quantified using similar measures, given by

$$S_{A,B,diff,phase}(f) = \left| \angle S_{AB,ref}(f) - \angle S_{AB,tumor}(f) \right|, \quad (4)$$

$$MD_{A,B,phase} = \frac{\left[\sum_{f=\Delta f}^{N\Delta f} S_{AB,diff,phase}(f) \right]}{N}. \quad (5)$$

The results for $MD_{A,B,amplitudes}$ for different transmitting and receiving antennas pairs are shown in Figure 3(a) and (d). The case for both the transmitting and receiving antennas that are vertically-oriented is shown in Figure 3(a). The vertical and horizontal axis corresponds to the transmitting and receiving antenna elements respectively, ranging from 1 to 18, with antenna element 1 locate at $\varphi = 0°$. The results for the cases of (i) transmitting using vertically-oriented antennas and receiving using horizontally-oriented antennas, (ii) transmitting using horizontally-oriented antennas and receiving using vertically-oriented antennas and (iii) transmitting using vertically-oriented and measuring using

horizontally-oriented antennas, are shown in Figures 3(b) to (d) respectively.
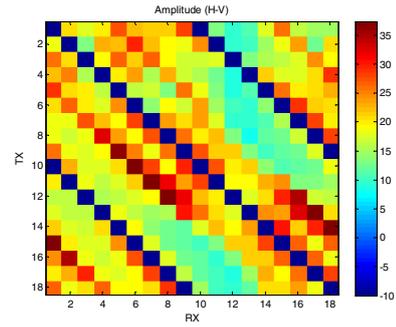
Figure 4. $MD_{A,B,amplitudes}$ values for the case of the 10mm tumor for A and B ranges from 1 to 18, with 1 corresponds to the position of $\varphi = 0°$. The transmitting antennas are horizontally-oriented and the receiving antennas are vertically-oriented.The values on the diagnols and the two second diagnoals are removed and artifically replaced by -10 shown in dark blue in the figures. The replaced values are for display purposes and should not be considered in the analysis.
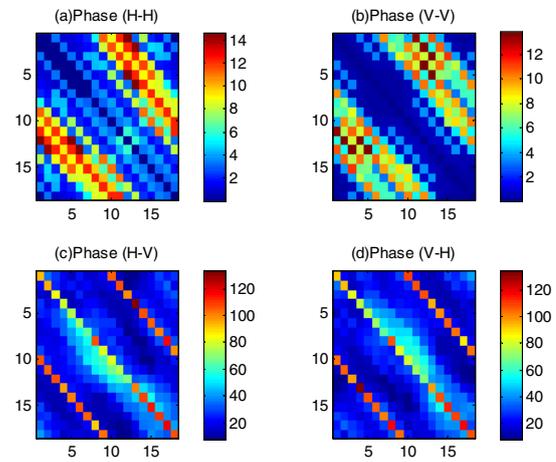
Figure 5. $MD_{A,B,phase}$ values for the case of the 10mm tumor for A and B ranges from 1 to 18, with antenna 1 corresponds to the position of $\varphi = 0°$. (a) to (d) shows the results with different transmitting and receiving antenna pairs that are oriented in (a)Horizontal_Horizontal, (b) Vertical_Vertical, (c) Horizontal_Vertical and (d) Vertical_Horizontal manners.

For the case when both transmitting and receiving antennas are located vertically or horizontally, the differences are relatively small with maximum $MD_{A,B,amplitudes}$ values up to 8% to 13% (as shown in Figure 3(a) and (b)). It is interesting to see that the relatively large values (shown as red color) appear in the two second diagonals of the figures, which correspond to the direct path. The diagonal component, which corresponds to the monostatic responses, appears to be relatively small for both cases. This is different to the results in our previous study [7] that maximum values occur along the diagonal when the scattered far fields are considered. The difference is due to the introduction of cross dipole elements in the near-field region where mutual coupling between the

antennas and higher order interactions between the breast and the antennas are taken into account. Further investigations are required to find out the reasons behind such differences.
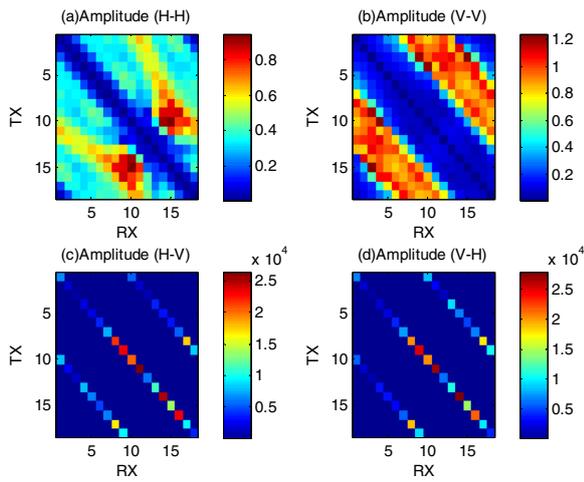
Figure 6. $MD_{A,B,amplitudes}$ values for the case of the 5mm tumor for A and B ranges from 1 to 18, with antenna 1 corresponds to the position of $\varphi = 0°$. (a) to (d) shows the results with different transmitting and receiving antenna pairs that are oriented in (a)Horizontal_Horizontal, (b) Vertical_Vertical, (c) Horizontal_Vertical and (d) Vertical_Horizontal manners.

Next, the cross pairs are considered and the corresponding results are shown in Figure 3(c) and (d). The results show that extremely large values (with more than 10,000%) appear in the off-diagonal and the two second diagonals that correspond to the cross monostatic responses and direct paths responses respectively. Such high values could be due to the fact that the geometry is symmetric for the case when there is no tumor such that the response is extremely low for those cases [7]. This is not realistic in practice as human breast is not homogenous. For other antenna pairs shown in Figures 3(c) and (d), the $MD_{A,B,amplitudes}$ values are within 10% to 35%. To get a better idea about the other antenna pairs, we have removed those large values on the diagonals and two second diagonals and replaced by a value of -10. The corresponding results for the (H-V) combination are shown in Figure 4. The deep blue color in the figure corresponds to the removed values and replaced artificially by -10. These values should not be considered in the analysis. Ignoring the removed values, it is seen that the the $MD_{A,B,amplitudes}$ values are from 15% to 35% which are higher than that of the cases with both transmitting and receiving antennas oriented in the same manner. Due to the reciprocity of electromagnetic waves, the results for V-H are also within the range of 15% to 35% and thus not included here.

Figure 5 shows the $MD_{A,B,phase}$ values. For the cases where both transmitting and receiving antennas are located in the same manner, the phase changes is within $15°$. For the cross antennas pairs, the large phase values occur at the diagonal and two off-diagonals with more than $100°$ phase changes.
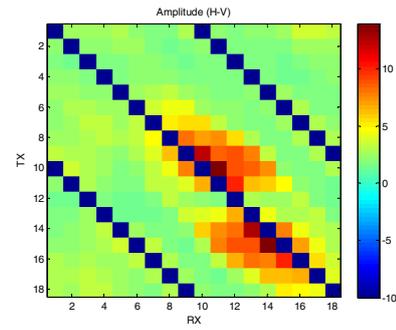
Figure 7. $MD_{A,B,amplitudes}$ values for the case of the 5mm tumor for A and B ranges from 1 to 18, with 1 corresponds to the position of $\varphi = 0°$. The transmitting antennas are horizontally-oriented and the receiving antennas are vertically-oriented.The values on the diagnoals and the two second diagnoals are removed and artifically replaced by -10 shown in dark blue in the figures. The replaced values are for display purposes and should not be considered in the analysis.

Figure 8. $MD_{A,B,phase}$ values for the case of the 5mm tumor for A and B ranges from 1 to 18, with antenna 1 corresponds to the position of $\varphi = 0°$. (a) to (d) shows the results with different transmitting and receiving antenna pairs that are oriented in (a)Horizontal_Horizontal, (b) Vertical_Vertical, (c) Horizontal_Vertical and (d) Vertical_Horizontal manners.

Next, the size of the tumor is now reduced to a 5mm radius sphere in the simulation and the corresponding results are shown in Figures 6 to 8. As the tumor size reduces, the contrast of the forward data reduced significantly for all cases. This is in line with the conclusion in our previous work that the data contrast is sensitive to the changes of tumor sizes [7]. Comparing the H-H, V-V cases with the H-V and V-H cases, the former two show the maximum $MD_{A,B,amplitudes}$ of 1 to 1.2% (Figure 6(a) and (b)), while that of the H-V case is within 5 to 15% (Figure 7). This indicates that potentially the cross-components could be useful for imaging small-sized tumor.

(a)Mean S parameters

(b)Minimum S parameters
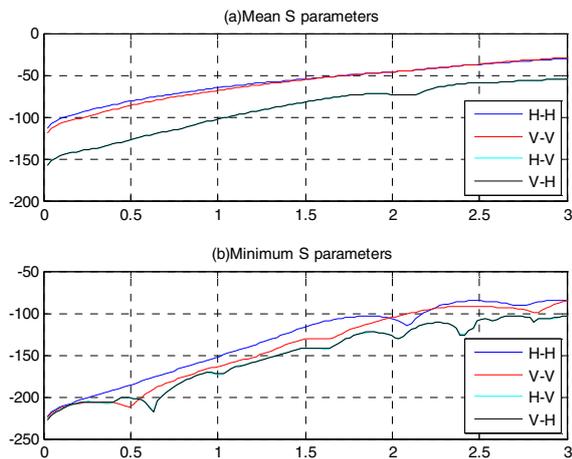
Figure 9.   Mean and Minumum values of the S-parameters at each frequency point for the 4 antenna confrigurations. The results here correspodn to the case of the breast volume with 5mm tumor.

(a)Mean S parameters

(b)Minimum S parameters
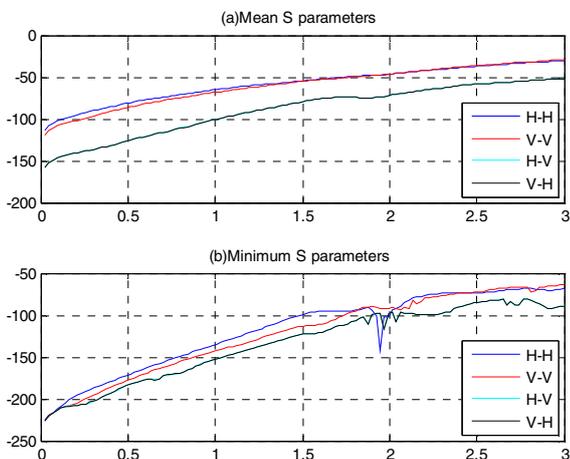
Figure 10. Mean and Minumum values of the S-parameters at each frequency point for the 4 antenna confrigurations. The results here correspond to the case of the breast volume with 10mm tumor.

Lastly, it is of practical interest about the level of the S-parameters at the antenna terminals. This tells us if we are able to measure those signals. The mean and minimum values of the S-parameters as a function of frequency are computed and shown in Figure 9 and 10. Here, the mean values are obtained by taking all the 18 by 18 antenna combinations into consideration for each of the four configurations (H-H, V-V, V-H and H-V) considered above. In general the S-parameters for H-H and V-V cases are higher than the V-H and H-V cases. The frequency response below 500MHz corresponds mainly to the breast volume [6] and thus it is not of significant interest as the objective here is to detect the tumor. Considering the minimum values of the S-parameters (Figure 9(b) and 10(b)), however, they are all below -90dB and -70dB

for the case with 5mm and 10mm tumor respectively. With the current state-of-art of vector network analyzer, we are able to measure signals accurately to -130dB, which indicates that we are able to measure the frequency response for the 10mm tumor down to around 1GHz and 1.5GHz for the 10mm tumor and 5mm tumor respectively.

IV.   CONCLUSIONS

The vectorial nature of electromagnetic scattering needs to be taken into consideration in three-dimensional microwave tomography problem. The motivation behind such needs and solutions for evaluating the quality of the forward data is proposed. Numerical examples of the forward scattering data evaluation have shown that better data contrast can be obtained when the cross antenna pairs are considered. The mean and minimum values of the S-parameters are also computed and found that the signal level increases as the frequency increases up to 3GHz. Using network analyzer, the frequency response between 1.5GHz to 3GHz can be accurately measured. Future work can be focus on the use of different antenna elements and matching liquid that could potentially improve the performance of the system.

REFERENCES

[1]   E. C. Fear, S. C. Hagness, P. M Meaney, M. Okoniewski and M. A. Stuchly, "Enhancing Breast Tumor Detection with Near-Field Imaging", *IEEE Microwave Magazine*, Vol. 48, pp. 48-56, Mar. 2002

[2]   A. Fhager and M. Persson, "Using a priori Data to Improve the Reconstruction of Small Objects in Microwave Tomography", *IEEE Trans. Microwave Theory and Techniques* , Vol. 55, No. 11, pp. 2454-2462, Nov. 2007

[3]   A. Fhager, *Microwave tomography*, Ph. D dissertation, Department of Signals and Systems, Chalmers University of Technology, Göteborg, Sweden, 2006.

[4]   W. -M. Boerner, M. B. Er-Arini, C. –Y. Chan and P. M. Mastrois, " Polarization Dependence in Electromagnetic Inverse Problem", *IEEE Trans. Antennas Propag.*, Vol. AP. 29, No. 2, pp. 262-271,March 1981

[5]   H. Mott, Remote Sensing with Polarmetric Radar, Wiley, 2007

[6]   H. S. Lui, A. Fhager, M. Persson, "Analysis of Forward Scattering Data for Microwave Breast Imaging", *Asia Pacific Microwave Conference*, Melbourne, Australia, 5-8 December 2011

[7]   H. S. Lui, A. Fhager, M. Persson, "On the Forward Scattering of Microwave Breast Imaging", (Special Issue on "Microwvae Imaging and Emerging Application), *International Journal of Biomedical Imaging*, in press.

[8]   FEKO EM Software & Systems S.A., (Pty) Ltd, 32 Techno Lane, Technopark, Stellenbosch, 7600, South Africa

[9]   S. C. Hagness, A. Taflov and J. E. Bridges, "Two-Dimensional FDTD Analysis of a Pulsed Microwave Confocal System for Breast Cancer Detection: Fixed-Focus and Antenna-Array Sensor", *IEEE Trans. Biomedical Engineering*, Vol. 45, no. 12, pp. 1470-1479, Dec. 1998